Partially $\mathcal{PT}$-symmetric lattice solitons in quadratic nonlinear media

Mahmut Bağcı*

Department of Software Development, School of Applied Sciences, Yeditepe University, Atasehir 34755, Istanbul, Turkey

(Received 24 September 2020; accepted 12 February 2021; published 24 February 2021)

Partially parity-time-symmetric (p$\mathcal{PT}$-symmetric) lattice solitons are explored in quadratic nonlinear media. The solution of the model a nonlinear Schrödinger (NLS) equation with coupling to a mean term and an additional external potential, is computed by modern numerical methods, and it is shown that p$\mathcal{PT}$-symmetric lattice solitons can exist in quadratic nonlinear media. The study concentrates on effects generated by the variation of lattice depth and quadratic nonlinearity strength that specify characteristics of the model, and the stability of the model is examined comprehensively by the nonlinear evolution and linear stability spectra of the solitons. It is demonstrated that stable evolution of solitons in a quadratic nonlinear media is possible for self-focusing p$\mathcal{PT}$-symmetric lattices. Moreover, it is observed that, for the defocusing case of the lattice, fundamental solitons decay into radiation modes, and the decay of these solitons can be delayed by a deeper potential.

DOI: 10.1103/PhysRevA.103.023530

I. INTRODUCTION

Solitons are localized waves that maintain their form and velocity during propagation because of a delicate balance between nonlinear and dispersive effects in the medium. Generation of solitons in nonlinear systems with real external potentials (lattices) have drawn much attention over the last two decades [1–12]. It is known that the external potential of complex optical systems can be richer than a real lattice when the optical system includes energy gain and loss, the potential of the medium would be complex [13] and in such systems, balanced gain and loss results in dissipative solitons [14–16].

In 1998, a novel theoretical approach was proposed by Bender and Boettcher [17] to show that non-Hermitian Hamiltonians can produce entirely real spectra when they possess parity-time ($\mathcal{PT}$) symmetry, where $\mathcal{PT}$ symmetry means that a Hamiltonian is invariant under complex conjugation and simultaneous reflection in all spatial directions [$V^*(x, y) = V(-x, -y)$] [13,18]. This pioneering exploration indicates the possibility of stable pulse propagation in $\mathcal{PT}$-symmetric optical systems [19] and triggered much research related to wave dynamics in $\mathcal{PT}$-symmetric potentials [20–30]. Furthermore, it was demonstrated that $\mathcal{PT}$-symmetric lattices can be realized both theoretically [18,31,32] and experimentally [33–36].

More recently, it was shown that, when a potential invariant under complex conjugation and reflection in a single spatial direction [i.e., $V^*(x, y) = V(-x, y)$ or $V^*(x, y) = V(x, -y)$], the linear spectrum can still be all real [37,38]. This special class of complex potentials is called "partially $\mathcal{PT}$ symmetric" (p$\mathcal{PT}$ symmetric). The existence and stability of multidimensional solitons in such lattices have been demonstrated by Yang [38]. Vortex solitons in p$\mathcal{PT}$-symmetric azimuthal potentials have been introduced in Ref. [39] and the existence and stability of gap solitons have been investigated in Ref. [40]. More importantly, symmetry breaking of solitons, which is forbidden for $\mathcal{PT}$-symmetric potentials, have been demonstrated in a special class of one-dimensional (1D) and two-dimensional (2D) p$\mathcal{PT}$-symmetric potentials [25,37]. Symmetry breaking can occur above a critical power, and this power threshold is a bifurcation point where the stability properties of the base branch is changed. On the bifurcated branch non-$\mathcal{PT}$-symmetric (asymmetric) solitons can exist, and they exhibit interesting stability dynamics, which are not observed in conservative systems, such as stable non-$\mathcal{PT}$-symmetric solitons (in 1D) and oscillatory instability or nonreciprocal nonlinear evolutions by spatial mirror reflection (in 2D).

In the studies mentioned, pulse dynamics are governed by nonlinear Schrödinger (NLS) type equations in cubic nonlinear media. However, it is known that, in many optical applications, the leading order polarization effect is quadratic [41–48]. In this study, the numerical existence of fundamental solitons in quadratic nonlinear media with p$\mathcal{PT}$-symmetric lattices are demonstrated and a detailed stability analysis is performed for the solitons obtained. The model for propagation of light beams in quadratic nonlinear media with a p$\mathcal{PT}$-symmetric lattice is given by a NLS equation with coupling to a mean term (denoted "NLSM systems") and an additional external potential.

The NLSM equations first obtained by Benney and Roskes in 1969 [49] were for water of finite depth, and the evolution of a three-dimensional (3D) wave packet in water of finite depth was investigated by Davey and Stewartson [50] in 1974. In 1975, the integrability of NLSM systems was studied by Ablowitz and Haberman [51], and in 1997 Ablowitz *et al.* [52–54] demonstrated that the evolution of the electromagnetic field in quadratic nonlinear media can be described by NLSM-type equations. Recently, wave collapse in the NLSM system was studied in Ref. [55], and wave collapse in the

*bagcimahmut@gmail.com

NLSM system was arrested by self-rectification [56] and real periodic external lattices [47]. The general NLSM system is given by [53,54,56]

$$iu_z + \Delta u + |u|^2 u - \rho u\phi = 0, \quad \phi_{xx} + \nu\phi_{yy} = (|u|^2)_{xx}, \quad (1)$$

where $u(x, y)$ is the normalized amplitude of the envelope of the normalized static electric field propagating in the z direction. $\Delta u \equiv u_{xx} + u_{yy}$ corresponds to diffraction, and the cubic term in u originates from the nonlinear (Kerr) change of the refractive index. The parameter ρ is a coupling constant that comes from the combined optical rectification and electro-optic effects modeled by the $\phi(x, y)$ field, and ν is the coefficient that comes from the anisotropy of the material.

The paper is outlined as follows: In Sec. II, the governing equations (model) for the quadratic nonlinear media with an external potential is presented and p$\mathcal{PT}$-symmetric lattice solitons are obtained by numerical solution of the model. In Sec. III, the stability of the lattice solitons is examined by the nonlinear evolution and linear stability spectra of the model. A brief summary of the numerical results is outlined in Sec. IV.

II. THE MODEL

Wave propagation in quadratically nonlinear media with an external potential is characterized by the following $(2 + 1)$-dimensional model

$$iu_z + \Delta u + |u|^2 u - \rho u\phi + V(x, y)u = 0,$$
$$\phi_{xx} + \nu\phi_{yy} = (|u|^2)_{xx}. \quad (2)$$

$V(x, y)$ is an external optical potential that is defined as follows for the model considered:

$$V(x, y) = V_0\{3(e^{-(x-x_0)^2-(y-y_0)^2} + e^{-(x+x_0)^2-(y-y_0)^2})$$
$$+ 2(e^{-(x-x_0)^2-(y+y_0)^2} + e^{-(x+x_0)^2-(y+y_0)^2})$$
$$+ iW_0[2(e^{-(x-x_0)^2-(y-y_0)^2} - e^{-(x+x_0)^2-(y-y_0)^2})$$
$$+ (e^{-(x-x_0)^2-(y+y_0)^2} - e^{-(x+x_0)^2-(y+y_0)^2})]\}, \quad (3)$$

where V_0 is the depth of the potential and $W_0 \geqslant 0$ is the depth of the potential's imaginary part (gain-loss component) [38]. Distances between humps of the potential are determined by x_0 and y_0 and are fixed to 1.5. The potential $V(x, y)$ fulfills the condition $V^*(x, y) = V(-x, y)$, so it is p$\mathcal{PT}$ symmetric. The lattice potentials with the focusing nonlinearity ($V_0 > 0$) and the defocusing nonlinearity ($V_0 < 0$) will be considered. The top view and cross-sectional shape of the potential $V(x, y)$ are plotted in Fig. 1 for $V_0 = 1$ and $W_0 = 0.1$.

The optical systems with $\mathcal{PT}$-symmetric lattices have a phase-transition point where the linear spectrum is all real below this threshold and partially complex above this threshold. This threshold has been determined as $W_0 = 2.14$ for the potential (3) considered in Ref. [38]. Therefore, when $W_0 < 2.14$ the spectrum is all real, and if W_0 exceeds 2.14, a phase transition occurs and the spectrum includes eigenvalues with nonzero imaginary parts.

A. Numerical solution for the model

The fundamental soliton solutions of model (2) is computed by the spectral renormalization (SR) method, which was developed by Ablowitz and Musslimani [57]. The SR method is based on a fixed-point iteration scheme. The essence of the method is to transform the governing equation into Fourier space and find a nonlinear nonlocal integral equation coupled to an algebraic equation.

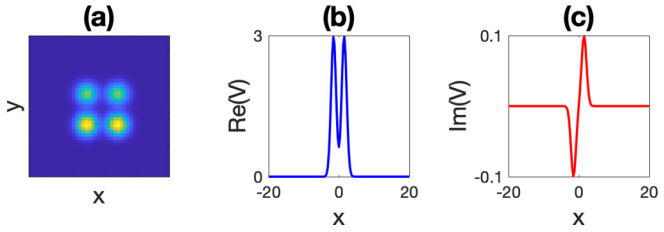

FIG. 1. (a) Top view of the p$\mathcal{PT}$-symmetric lattice. Cross section along the x axis of (b) the real part, and (c) the imaginary part of the lattice when $V_0 = 1$ and $W_0 = 0.1$.

The ansatz $u(x, y, z) = f(x, y)e^{i\mu z}$ is used to get a solution of the NLSM model (2). Here, $f(x, y)$ is a complex-valued function and μ is the propagation constant (or eigenvalue). Upon inserting the ansatz into the model (2), the following eigen-equation is obtained:

$$-\mu f + \Delta f + |f|^2 f - \rho f\phi + V(x, y)f = 0,$$
$$\phi_{xx} + \nu\phi_{yy} = (|f|^2)_{xx}. \quad (4)$$

Applying a Fourier transform to Eq. (4) gives

$$-\mu\hat{f} - (k_x^2 + k_y^2)\hat{f} + \mathcal{F}[|f|^2 f - \rho f\phi + V(x, y)f] = 0,$$
$$(k_x^2 + \nu k_y^2)\hat{\phi} = k_x^2\mathcal{F}[|f|^2], \quad (5)$$

where $\mathcal{F}$ denotes the Fourier transform [$\mathcal{F}(f) = \hat{f}$] and $\vec{k} = (k_x, k_y)$ are Fourier variables. To circumvent a possible singularity in the denominator when $\mu < 0$, a term $r\hat{f}$ is added to and subtracted from the system (5),

$$[\mu + |\vec{k}|^2]\hat{f} + r\hat{f} - r\hat{f} = \mathcal{F}[|f|^2 f - \rho f\phi + V(x, y)f],$$
$$(k_x^2 + \nu k_y^2)\hat{\phi} = k_x^2\mathcal{F}[|f|^2], \quad (6)$$

where r is a positive constant and $|\vec{k}|^2 = k_x^2 + k_y^2$. After this operation, $\hat{f}$ and $\hat{\phi}$ can be calculated as follows:

$$\hat{f} = \frac{\mathcal{F}[|f|^2 f - \rho f\phi + V(x, y)f + (r - \mu)f]}{r + |\vec{k}|^2},$$
$$\hat{\phi} = \frac{k_x^2}{k_x^2 + \nu k_y^2}\mathcal{F}[|f|^2]. \quad (7)$$

A new field variable $f(x, y) = \lambda w(x, y)$ is introduced to avoid collapse (or blowup) of the solution's amplitude under iterations. $\lambda \neq 0$ is a constant to be determined. Substituting new field variables into the Eqs. (7) gives

$$\hat{w}_{n+1} = \frac{\mathcal{F}[|\lambda_n|^2|w_n|^2 w_n - \rho w_n\phi_n + V(x, y)w_n + (r - \mu)w_n]}{r + |\vec{k}|^2},$$
$$\hat{\phi}_n = \frac{k_x^2}{k_x^2 + \nu k_y^2}|\lambda_n|^2\mathcal{F}[|w_n|^2]. \quad (8)$$

Let $\hat{\phi}_n = |\lambda_n|^2\hat{\Phi}_n$, then, multiplying the first equation in system (8) by $\hat{w}_n^*$ and integrating over the entire space (x, y), the

renormalization parameter $|\lambda_n|$ is determined as follows:

$$|\lambda_n|^2 = \frac{\int_{-\infty}^{\infty}\int_{-\infty}^{\infty}\{(|\vec{k}|^2+\mu)|\hat{w}_n|^2 - \mathcal{F}[Vw_n]\hat{w}_n^*\}dk_x dk_y}{\int_{-\infty}^{\infty}\int_{-\infty}^{\infty}\{\mathcal{F}[|w_n|^2 w_n - \rho w_n \Phi_n]\hat{w}_n^*\}dk_x dk_y},$$
$$\Phi_n = \mathcal{F}^{-1}\left[\frac{k_x^2}{k_x^2+\nu k_y^2}\mathcal{F}[|w_n|^2]\right]. \quad (9)$$

The iteration continues until the relative error $\lambda_{\text{error}} = |\lambda_{n+1}/\lambda_n - 1| < 10^{-10}$. It has been demonstrated that this algorithm converges rapidly for a wide-range of nonlinear partial differential equations [58–60]. Thus, the numerical solutions (fundamental solitons) of the model (2) are obtained from a convergent iterative scheme. The algorithm usually converges to the solution within less than 100 iterations when suitable parameter values are chosen for the model. The constant r is chosen heuristically and in most of the cases it can be selected from a wide interval such as any natural number between 5 and 20. It should be noted that increasing the value of r slows down the convergence of the algorithm. The initial condition of the SR algorithm is a typical Gaussian given by

$$w_0(x, y) = e^{-\left[(x-x_0)^2+(y-y_0)^2\right]}, \quad (10)$$

where x_0 and y_0 represent the location of the solution on the lattice.

B. The fundamental solitons

Using the SR method, the numerical solution of the model (2) is computed. The initial condition of the algorithm is focused on the center of lattice by setting $x_0 = y_0 = 0$ in Eq. (10), and this location is a local minimum of the p$\mathcal{PT}$-symmetric potential (see Fig. 1). Unless otherwise specified, we set parameters in the model (2) as follows:

$$(\rho, \nu, W_0) = (0.1,\ 1,\ 0.1). \quad (11)$$

With these parameters, the SR algorithm converges to a soliton solution of the model (2) in both self-focusing ($V_0 = 1$) and defocusing ($V_0 = -1$) regimes of $\mathcal{PT}$-symmetric lattices. The top view and diagonal cross sections of the real and imaginary part of the fundamental soliton is shown in Fig. 2 for $V_0 = -1$, $\mu = 1.7$, and $r = 15$. Note that fundamental solitons can be generated by the model (2) for $0 \leqslant \rho \leqslant 1.2$ and $0 \leqslant \nu$ when $V_0 = -1$, $W_0 = 0.1$. Similarly, for the self-focusing ($V_0 > 0$) case of the lattice, double-hump soliton solutions can be obtained when $V_0 = 1$ and $W_0 = 0.1$ for $0 \leqslant \rho \leqslant 1.8$, $0 \leqslant \nu$. Such a double-hump soliton is shown in Fig. 3.

Furthermore, if the initial condition (10) is focused to any local maximum of the lattice (i.e., $x_0 = \pm 1.5$ and $y_0 = \pm 1.5$), the algorithm converges to double-hump stationary solutions when $V_0 > 0$, and when $V_0 < 0$ the convergence cannot be satisfied and the solution drifts away from the lattice maximum to nearby lattice minima.

III. STABILITY ANALYSIS

The SR method is used to calculate soliton solutions of the model (2). Once the solution is obtained, the stability of solitons can be explored. The linear stability of solitons are examined by the spectrum of linearization operator near the fundamental soliton and the nonlinear stability of the solitons are investigated by direct simulation of the nonlinear model.

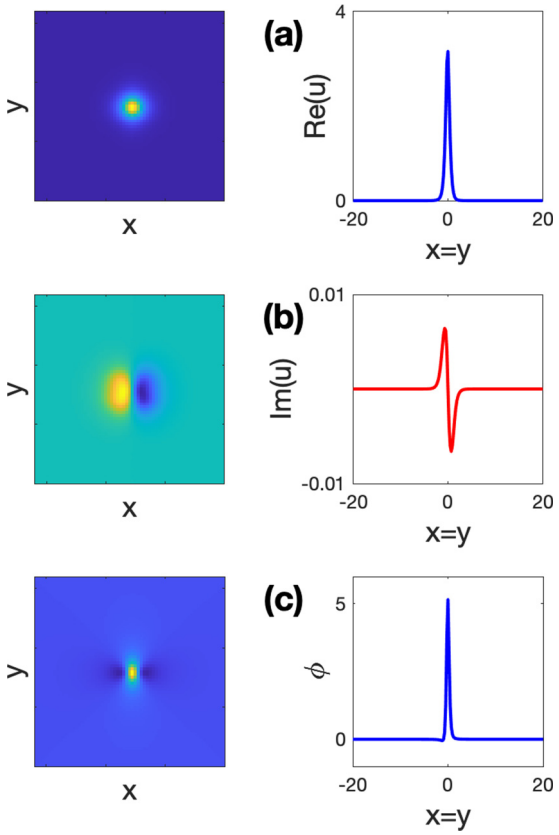

FIG. 2. Fundamental soliton located at the center of the p$\mathcal{PT}$-symmetric lattice for the parameters given in Eq. (11). (a) Top view (left) and diagonal cross section (right) for the real part of the soliton. (b) Top view (left) and diagonal cross section (right) for imaginary part of the soliton. (c) Top view (left) and diagonal cross-section (right) of the coupled field ϕ.

A. Linear stability of the fundamental solitons

To examine linear stability of the model (2), we calculate the spectrum of linearization of the model near the solitons

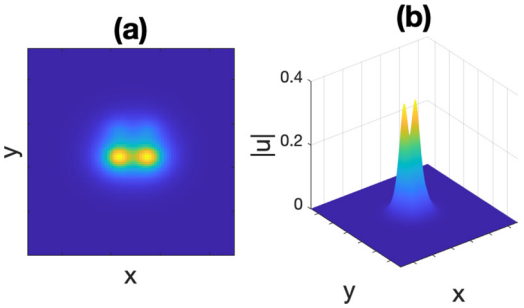

FIG. 3. Soliton solution of self-focusing p$\mathcal{PT}$-symmetric lattice when $V_0 = 1$ and $\mu = 0.83$. (a) Top view and (b) 3D view of the double-hump soliton.

that are obtained with the SR method. By denoting

$$U = e^{i\mu z}[u_0(x, y) + \tilde{u}(x, y, z)], \tag{12}$$

where $u_0(x, y)$ is the fundamental soliton, μ is the propagation constant and $\tilde{u} \ll 1$ is the infinitesimal perturbation. If the perturbation $\tilde{u}$ decays to zero, then the soliton is considered to be linearly stable. Inserting the perturbed solution U into the model (2), we get the linearized system for $\tilde{u}$ by neglecting small terms of second order $[O(\tilde{u}^2)]$:

$$\tilde{u}_z = -i\mu\tilde{u} + i\Delta\tilde{u} + i\left(2|u_0|^2\tilde{u} + u_0^2\tilde{u}^*\right) - i\rho\phi\tilde{u} + iV\tilde{u}. \tag{13}$$

Upon separating the fundamental soliton u_0 and the perturbation $\tilde{u}$ into real and imaginary parts as follows:

$$u_0 = a + ib, \quad \tilde{u} = Re^{\lambda z} + iIe^{\lambda z}, \tag{14}$$

we obtain $\tilde{u}_z = \lambda\tilde{u}$, where λ is the growth rate of disturbance. Substituting u_0 and $\tilde{u}$ into the system (13) results in the eigenvalue problem

$$\mathbf{AV} = \lambda\mathbf{V}, \tag{15}$$

where

$$\mathbf{A} = \begin{pmatrix} F_R & G_I \\ G_R & F_I \end{pmatrix}, \quad \mathbf{V} = \begin{pmatrix} R \\ I \end{pmatrix}.$$

The matrix coefficients of $\mathbf{A}$ are given by

$$\begin{aligned} F_R &= -2ab, \\ G_I &= -[\Delta + (a^2 + 3b^2) - \mu - \rho\phi + V], \\ F_I &= 2ab, \\ G_R &= [\Delta + (3a^2 + b^2) - \mu - \rho\phi + V]. \end{aligned} \tag{16}$$

The eigenvalues of $\mathbf{A}$ can be calculated numerically with finite difference discretization of the spatial domain. If any eigenvalue in the spectrum has a positive real part, the solution is linearly unstable.

The power, which is defined by $\mathrm{P} = \int\int_{-\infty}^{\infty} |u|^2 dxdy$, plays an important role in determining the stability properties of the solitons. Therefore, the power-eigenvalue diagram of gap solitons are investigated in detail by the variation of V_0 and ρ parameters in Fig. 4. Here, the linear stability (solid blue) and instability (red dotted) regions are determined by computation of eigenvalue spectra for each point on the power curves. It is important to note that this analysis shows the first band-gap boundaries for the considered parameter regimes in each panel. For instance, when $\rho = 0.1$ and $V_0 = 1$, the soliton solutions can be obtained for $\mu \in [0.78, 0.1.74]$ within the gap region [see Fig. 4(c)]. When $V_0 = 1$, the solitons are linearly stable below a critical power ($P_c = 1.73$) in both $\rho = 0$ and $\rho = 0.1$ cases [see Figs. 4(a) and 4(c)], and the solitons are stable for $V_0 = -1$ and $\rho = 0$ when their power is greater than 11.38 [see Fig. 4(b)]. The solitons are unstable at each point of the power curve when $V_0 = -1$ and $\rho = 0.1$ [see Fig. 4(d)].

The solitons that are shown in Figs. 2 and 3 correspond to points "d" and "c" in Figs. 4(d) and 4(c), respectively. This fact reveals the linear stability of the soliton (at point c) when $\mu = 0.83$ and $V_0 = 1$ and the linear instability of the soliton (at point d) when $\mu = 1.7$ and $V_0 = -1$. Furthermore, when $V_0 = 1$, the solitons are found to be linearly stable for $0 \leqslant \rho \leqslant 0.9$ and $0 \leqslant \nu$, and it is observed that, as ρ increases, the soliton power increases, whereas the power decreases with the increase of the parameters ν, V_0, and W_0.

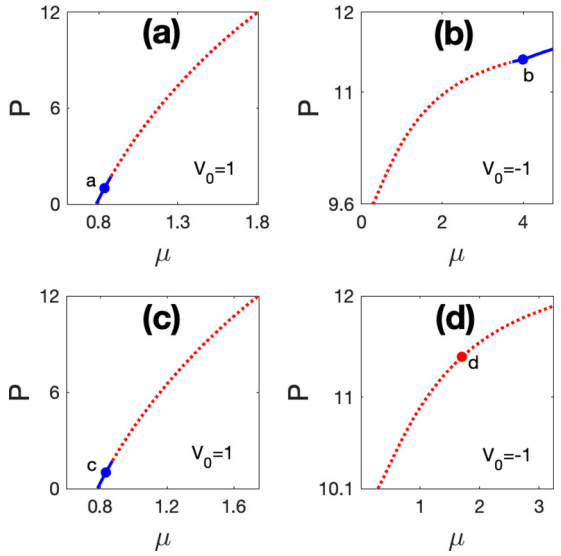

FIG. 4. The power diagram of solitons when (a) $\rho = 0$, $V_0 = 1$; (b) $\rho = 0$, $V_0 = -1$; (c) $\rho = 0.1$, $V_0 = 1$; and (d) $\rho = 0.1$, $V_0 = -1$. Solid blue and red dotted lines show stable and unstable regions for the gap solitons, respectively.

B. Nonlinear evolution of the fundamental solitons

The nonlinear stability of fundamental solitons are investigated by direct simulation of the model (2) for long times. A finite-difference discretization scheme is used in the spatial domain and the solution is advanced in z with a fourth-order Runge-Kutta method.

In Fig. 5, the linear spectrum (left panels) and nonlinear evolution (right panels) of the solitons are displayed. Here, the fundamental solitons, which are obtained at points "a," "b," "c," and "d" in Fig. 4, are used as the initial conditions of the evolution in Figs. 5(a)–5(d), respectively. As can be seen from Figs. 5(a)–5(c), the linear spectra of solitons that are obtained at points a–c are purely imaginary (none of their eigenvalues have a real part), and the peak amplitude of the evolved solitons oscillates over relatively small amplitudes during the propagation, thus stable evolution of the soliton can be achieved for the considered parameter regimes. On the other hand, the linear spectrum of the soliton, which is obtained at point d, involves an eigenvalue with positive real part, and peak amplitude of the evolved soliton decreases significantly during the evolution, which indicates instability of the examined soliton.

To see the effect of quadratic nonlinearity and of the depth of the p$\mathcal{PT}$-symmetric potential on the pulse stability, the linear spectrum (left panels) and nonlinear evolution (right panels) of unstable solitons are investigated for various ρ, ν, V_0, and W_0 values in Fig. 6. Here, for the first case of nonlinear evolution, the initial condition is chosen as the soliton at point d (shown by solid blue line) and the maximum real part of eigenvalues in the spectrum of this soliton [$\max(\lambda_{Re}) = 1.661$] is marked by a red circle in each spectrum. The evolution results show that, as the optical rectification

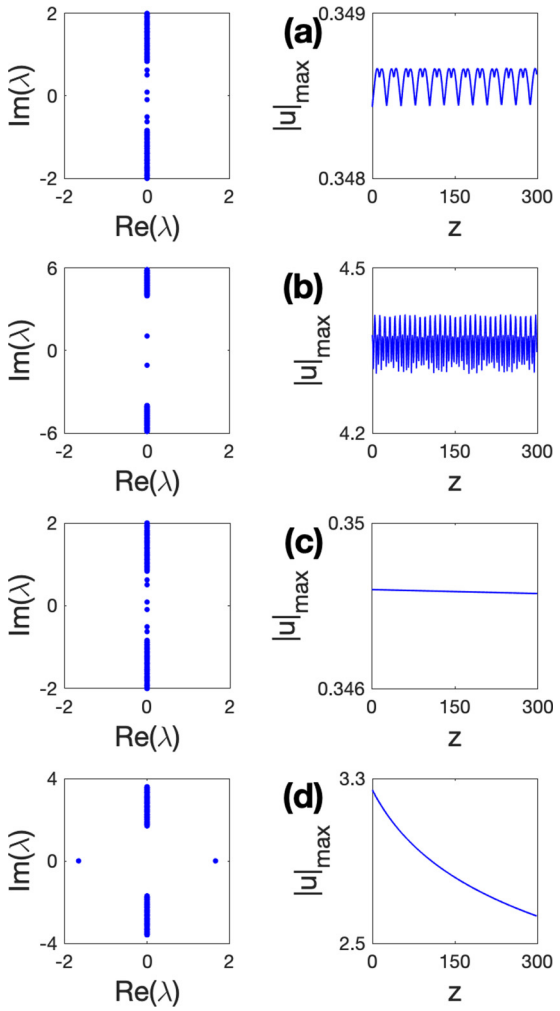

FIG. 5. The linear spectrum (left panel) and peak amplitude (right panel) of the evolved soliton from $z = 0$ to $z = 300$ (a) when $V_0 = 1$, $\rho = 0$, and $\mu = 0.83$; (b) when $V_0 = -1$, $\rho = 0$, and $\mu = 4$; (c) when $V_0 = 1$, $\rho = 0.1$, and $\mu = 0.83$; and (d) when $V_0 = -1$, $\rho = 0.1$, and $\mu = 1.7$.

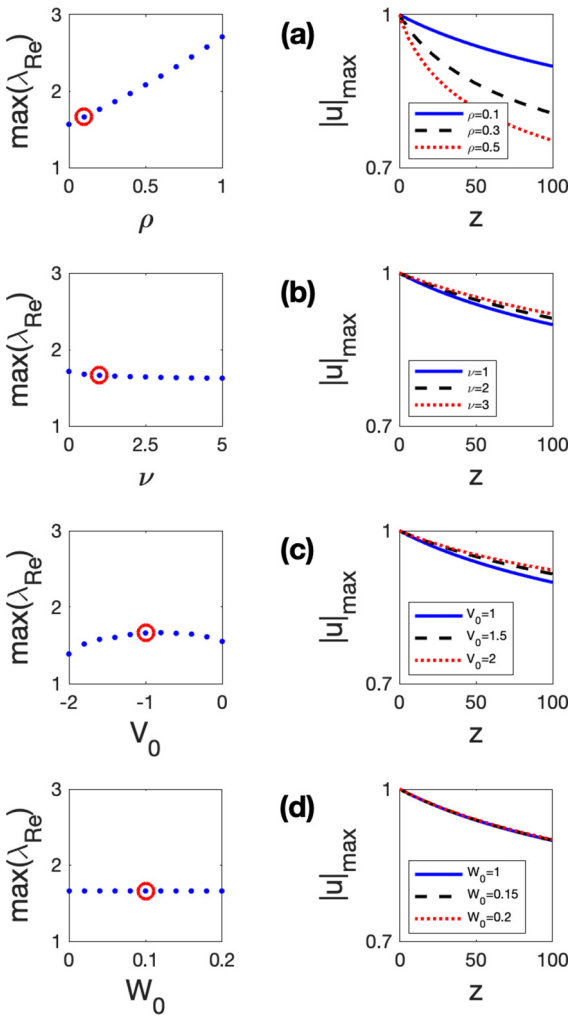

FIG. 6. The linear spectra (left panels) and peak amplitude of the evolved solitons (right panels) in the defocusing p$\mathcal{PT}$-symmetric potential. The fundamental soliton is obtained (a) for varied values of ρ when $\nu = 1$, $V_0 = -1$, and $W_0 = 0.1$; (b) for varied values of ν when $\rho = 0.1$, $V_0 = -1$, and $W_0 = 0.1$; (c) for varied values of V_0 when $\rho = 0.1$, $\nu = 1$, and $W_0 = 0.1$; and (d) for varied values of W_0 when $\rho = 0.1$, $\nu = 1$, and $V_0 = -1$.

parameter ρ increases, the propagation distance of the soliton decreases, and when $\rho > 0$, the solitons decay after a finite distance of propagation in each case [see Fig. 6(a)]. On the other hand, the increased anisotropy parameter ν and gain-loss component W_0 extend the propagation distance of the soliton [see Figs. 6(b) and 6(d)]. Importantly, as can be seen from Fig. 6(c), a deeper potential ($V_0 = 2$) delays decay of the soliton and extends the propagation distance. These results are also demonstrated by linear spectra of the solitons (left panels in Fig. 6). The spectral analysis shows that, when ρ increases, the maximum real part of the eigenvalues increases and none of the solitons are found to be linearly stable [see Fig. 6(a)], whereas the maximum real part of the eigenvalues is decreasing with increasing parameter ν [see Fig. 6(b)]. Although the maximal real part of the eigenvalues is increasing when potential depth $|V_0|$ increases from 0 to 1, beyond this point (when $|V_0| > 1$) it decreases (see Fig. 6(c)).

In light of the analysis, it is observed that the stability properties of the solitons are considerably altered by the coupling parameter ρ and the potential depth $|V_0|$, and the dynamics of the considered solitons are weakly effected by the variation of the anisotropy parameter ν and the depth of imaginary part W_0.

It should be noted that, although fundamental solitons can be generated when $\nu > 0$ (in semi-infinite interval) and increased values of ν extends the propagation distance of the solitons, it cannot be considered as a collapse-arrest mechanism since the parameters ρ and ν are fixed values that depend on the type of optical materials.

IV. CONCLUSIONS

The numerical existence of p$\mathcal{PT}$-symmetric lattice solitons are demonstrated in the quadratic nonlinear media, and stability properties in the lattices considered are explored by examining the nonlinear evolution and linear stability spectra of the solitons.

Stability analysis shows that, if the quadratic nonlinearity is absent ($\rho = 0$), solitons can be linearly stable in a wide range of parameter values where linear spectra of solitons include purely imaginary eigenvalues, and these solitons can stay nonlinearly stable during the evolution for both the self-focusing ($V_0 = 1$) and defocusing ($V_0 = -1$) case of the potential. Similarly, when $\rho > 0$, the solitons can be stable in the self-focusing potential ($V_0 = 1$) for a wide range of the parameters if their power is below a critical value. On the other hand, when $\rho > 0$ and $V_0 = -1$, the linear stability spectra of the solitons include eigenvalues with positive real part and none of the solitons can stay stable during nonlinear evolution in defocusing potential.

For unstable solitons, as the quadratic nonlinearity coefficient ρ is increased, the propagation distance of the evolved soliton is shortened, whereas the propagation distance of unstable solitons can be extended by increasing the potential depth ($|V_0|$).

In conclusion, the numerical results demonstrate that stable p$\mathcal{PT}$-symmetric lattice solitons can be obtained in quadratic nonlinear media for a suitable range of parameters, and although strong quadratic nonlinearity in the model impoverish the stability properties of the solitons, the instability due to the decay of the solitons' amplitude can be delayed by a deeper potential.

[1] D. N. Christodoulides, F. Lederer, and Y. Silberberg, Discretizing light behavior in linear and nonlinear waveguide lattices, Nature (London) **424**, 817 (2003).

[2] A. A. Sukhorukov, Y. S. Kivshar, H. S. Eisenberg, and Y. Silberberg, Spatial optical solitons in waveguide arrays, IEEE J. Quantum Electron. **39**, 31 (2003).

[3] N. K. Efremidis, J. Hudock, D. N. Christodoulides, J. W. Fleischer, O. Cohen, and M. Segev, Two-Dimensional Optical Lattice Solitons, Phys. Rev. Lett. **91**, 213906 (2003).

[4] J. W. Fleischer, M. Segev, N. K. Efremidis, and D. N. Christodoulides, Observation of two-dimensional discrete solitons in optically induced nonlinear photonic lattices, Nature (London) **422**, 147 (2003).

[5] D. Neshev, Y. S. Kivshar, H. Martin, and Z. Chen, Soliton stripes in two-dimensional nonlinear photonic lattices, Opt. Lett. **29**, 486 (2004).

[6] H. Buljan, G. Bartal, O. Cohen, T. Schwartz, O. Manela, T. Carmon, M. Segev, J. W. Fleischer, and D. N. Christodoulides, Partially coherent waves in nonlinear periodic lattices, Stud. Appl. Math. **115**, 173 (2005).

[7] H. Sakaguchi and B. A. Malomed, Gap solitons in quasiperiodic optical lattices, Phys. Rev. E **74**, 026601 (2006).

[8] Y. V. Kartashov, V. A. Vysloukh, and L. Torner, Soliton shape and mobility control in optical lattices, Prog. Opt. **52**, 63 (2009).

[9] M. J. Ablowitz, N. Antar, İ. Bakırtaş, and B. Ilan, Band-gap boundaries and fundamental solitons in complex two-dimensional nonlinear lattices, Phys. Rev. A **81**, 033834 (2010).

[10] M. J. Ablowitz, N. Antar, İ. Bakırtaş, and B. Ilan, Vortex and dipole solitons in complex two-dimensional nonlinear lattices, Phys. Rev. A **86**, 033804 (2012).

[11] M. Bağcı, İ. Bakırtaş, and N. Antar, Vortex and dipole solitons in lattices possessing defects and dislocations, Opt. Commun. **331**, 204 (2014).

[12] P. Naldesi, J. P. Gomez, B. Malomed, M. Olshanii, A. Minguzzi, and L. Amico, Rise and Fall of a Bright Soliton in an Optical Lattice, Phys. Rev. Lett. **122**, 053001 (2019).

[13] J. Yang, Necessity of $\mathcal{PT}$ symmetry for soliton families in one-dimensional complex potentials, Phys. Lett. A **378**, 367 (2014).

[14] N. Akhmediev and A. Ankiewicz, *Dissipative Solitons* (Springer, Berlin, 2005).

[15] D. A. Zezyulin, Y. V. Kartashov, and V. V. Konotop, Solitons in a medium with linear dissipation and localized gain, Opt. Lett. **36**, 1200 (2011).

[16] P. Grelu and N. Akhmediev, Dissipative solitons for mode-locked lasers, Nat. Photonics **6**, 84 (2012).

[17] C. M. Bender and S. Boettcher, Real Spectra in Non-Hermitian Hamiltonians having $\mathcal{PT}$ Symmetry, Phys. Rev. Lett. **80**, 5243 (1998).

[18] *Parity-Time Symmetry and Its Applications*, edited by D. N. Christodoulides and J. Yang (Springer, Singapore, 2018) .

[19] K. G. Makris, R. El-Ganainy, D. N. Christodoulides, and Z. H. Musslimani, Beam Dynamics in $\mathcal{PT}$ Symmetric Optical Lattices, Phys. Rev. Lett. **100**, 103904 (2008).

[20] Z. H. Musslimani, K. G. Makris, R. El-Ganainy, and D. N. Christodoulides, Optical Solitons in $\mathcal{PT}$ Periodic Potentials, Phys. Rev. Lett. **100**, 030402 (2008).

[21] F. K. Abdullaev, Y. V. Kartashov, V. V. Konotop, and D. A. Zezyulin, Solitons in $\mathcal{PT}$-symmetric nonlinear lattices, Phys. Rev. A **83**, 041805(R) (2011).

[22] N. V. Alexeeva, I. V. Barashenkov, A. A. Sukhorukov, and Y. S. Kivshar, Optical solitons in $\mathcal{PT}$-symmetric nonlinear couplers with gain and loss, Phys. Rev. A **85**, 063837 (2012).

[23] S. Nixon, L. Ge, and J. Yang, Stability analysis for solitons $\mathcal{PT}$-symmetric optical lattices, Phys. Rev. A **85**, 023822 (2012).

[24] D. Leykam, V. V. Konotop, and A. S. Desyatnikov, Discrete vortex solitons and parity time symmetry, Opt. Lett. **38**, 371 (2013).

[25] J. Yang, Symmetry breaking of solitons in one-dimensional parity-time-symmetric optical potentials, Opt. Lett. **39**, 5547 (2014).

[26] İ. Göksel, N. Antar, and İ. Bakırtaş, Solitons of (1+1)D cubic-quintic nonlinear Schrödinger equation with $\mathcal{PT}$-symmetric potentials, Opt. Commun. **354**, 277 (2015).

[27] S. V. Suchkov, A. A. Sukhorukov, J. Huang, S. V. Dmitriev, C. Lee, and Y. S. Kivshar, Nonlinear switching and solitons in $\mathcal{PT}$-symmetric photonic systems, Laser Photonics Rev. **10**, 177 (2016).

[28] Y. V. Kartashov, C. Hang, G. Huang, and L. Torner, Three-dimensional topological solitons in *PT*-symmetric optical lattices, Optica **3**, 1048 (2016).

[29] M. Bağcı, İ. Bakırtaş, and N. Antar, Fundamental solitons in parity-time symmetric lattice with a vacancy defect, Opt. Commun. **356**, 472 (2015).

[30] İ. Göksel, N. Antar, and İ. Bakırtaş, Two-dimensional solitons in $\mathcal{PT}$-symmetric optical media with competing nonlinearity, Optik (Munich, Ger.) **156**, 470 (2018).

[31] A. Ruschhaupt, F. Delgado, and J. G. Muga, Physical realization of $\mathcal{PT}$-symmetric potential scattering in a planar slab waveguide, J. Phys. A: Math. Gen. **38**, L171 (2005).

[32] K. G. Makris, R. El-Ganainy, D. N. Christodoulides, and Z. H. Musslimani, $\mathcal{PT}$-symmetric periodic optical potentials, Int. J. Theor. Phys. **50**, 1019 (2011).

[33] C. E. Rüter, K. G. Makris, R. El-Ganainy, D. N. Christodoulides, M. Segev, and D. Kip, Observation of parity–time symmetry in optics, Nat. Phys. **6**, 192 (2010).

[34] A. Regensburger, C. Bersch, M. A. Miri, G. Onishchukov, D. N. Christodoulides, and U. Peschel, Parity-time synthetic photonic lattices, Nature (London) **488**, 167 (2012).

[35] V. V. Konotop, J. Yang, and D. A. Zezyulin, Nonlinear waves in $\mathcal{PT}$-symmetric systems, Rev. Mod. Phys. **88**, 035002 (2016).

[36] L. Feng, R. El-Ganainy, and L. Ge, Non-Hermitian photonics based on parity–time symmetry, Nat. Photonics **11**, 752 (2017).

[37] J. Yang, Symmetry breaking of solitons in two-dimensional complex potentials, Phys. Rev. E **91**, 023201 (2015).

[38] J. Yang, Partially $\mathcal{PT}$ symmetric optical potentials with all-real spectra and soliton families in multidimensions, Opt. Lett. **39**, 1133 (2014).

[39] Y. V. Kartashov, V. V. Konotop, and L. Torner, Topological States in Partially-$\mathcal{PT}$-Symmetric Azimuthal Potentials, Phys. Rev. Lett. **115**, 193902 (2015).

[40] L. Ge, Gap Solitons in Partially Parity-Time-Symmetric Optical Lattices, in *Second International Conference on Photonics and Optical Engineering*, edited by C. Zhang and A. Asundi (SPIE, 2017), Vol. 10256, pp. 31–38.

[41] K. Hayata and M. Koshiba, Multidimensional Solitons in Quadratic Nonlinear Media, Phys. Rev. Lett. **71**, 3275 (1993).

[42] W. E. Torruellas, Z. Wang, D. J. Hagan, E. W. VanStryland, G. I. Stegeman, L. Torner, and C. R. Menyuk, Observation of Two-Dimensional Spatial Solitary Waves in a Quadratic Medium, Phys. Rev. Lett. **74**, 5036 (1995).

[43] R. Schiek, Y. Baek, and G. I. Stegeman, One-dimensional spatial solitary waves due to cascaded second-order nonlinearities in planar waveguides, Phys. Rev. E **53**, 1138 (1996).

[44] L. Torner and A. P. Sukhorukov, Quadratic solitons, Opt. Photonics News **13**, 42 (2002).

[45] A. V. Buryak, P. D. Trapani, D. V. Skryabin, and S. Trillo, Optical solitons due to quadratic nonlinearities: From basic physics to futuristic applications, Phys. Rep. **370**, 63 (2002).

[46] V. Lutsky and B. A. Malomed, One- and two-dimensional solitons supported by singular modulation of quadratic nonlinearity, Phys. Rev. A **91**, 023815 (2015).

[47] M. Bağcı, I. Bakırtaş, and N. Antar, Lattice solitons in nonlinear Schrödinger equation with coupling-to-a-mean-term, Opt. Commun. **383**, 330 (2017).

[48] M. Bağcı and J. N. Kutz, Spatiotemporal mode locking in quadratic nonlinear media, Phys. Rev. E **102**, 022205 (2020).

[49] D. J. Benney and G. J. Roskes, Wave instabilities, Stud. Appl. Math. **48**, 377 (1969).

[50] A. Davey and K. Stewartson, On three-dimensional packets of surface waves, Proc. R. Soc. A **338**, 101 (1974).

[51] M. J. Ablowitz and R. Haberman, Nonlinear Evolution Equations—Two and Three Dimensions, Phys. Rev. Lett. **35**, 1185 (1975).

[52] M. J. Ablowitz, G. Biondini, and S. Blair, Localized multidimensional optical pulses in non-resonant quadratic materials, Math. Comp. Simul. **56**, 511 (2001).

[53] M. J. Ablowitz, G. Biondini, and S. Blair, Multi-dimensional pulse propagation in non-resonant $\chi^{(2)}$ materials, Phys. Lett. A **236**, 520 (1997).

[54] M. J. Ablowitz, G. Biondini, and S. Blair, Nonlinear Schrödinger equations with mean terms in nonresonant multidimensional quadratic materials, Phys. Rev. E **63**, 046605 (2001).

[55] M. Ablowitz, İ. Bakırtaş, and B. Ilan, Wave collapse in a class of nonlocal nonlinear Schrödinger equations, Phys. D (Amsterdam, Neth.) **207**, 230 (2005).

[56] L.-C. Crasovan, J. P. Torres, D. Mihalache, and L. Torner, Arresting Wave Collapse by Wave Self-Rectification, Phys. Rev. Lett. **91**, 063904 (2003).

[57] M. J. Ablowitz and Z. H. Musslimani, Spectral renormalization method for computing self-localized solutions to nonlinear systems, Opt. Lett. **30**, 2140 (2005).

[58] M. J. Ablowitz, A. S. Fokas, and Z. H. Musslimani, On a new non-local formulation of water waves, J. Fluid Mech. **562**, 313 (2006).

[59] M. J. Ablowitz and T. P. Horikis, Solitons and spectral renormalization methods in nonlinear optics, Eur. Phys. J. Spec. Top. **173**, 147 (2009).

[60] N. Antar, Pseudospectral renormalization method for solitons in quasicrystal lattice with the cubic-quintic nonlinearity, J. Appl. Math. **2014**, 848153 (2014).